Analysis of Landsat-8 Images in Visible and Infrared Spectra

Ahmad Salehi[1], Niloofar Kalashtari[2]

[1]Master's students of Space Sciences and Technologies, University of Bremen, Germany

[2]Bachelor's student of Electrical Engineering, University of Guilan, Iran

Abstract

Landsat-8 is a satellite of the Landsat series dedicated to the Earth observation. It carries two instruments on-board that act as camera sensor to detect and process incoming light from the Earth. The two sensors called OLI and TIRS operate in visible and infrared parts of electromagnetic spectrum. Since every element on the Earth's surface and in the atmosphere reflects and emits radiation in its individual wavelength, it is possible to distinguish between the elements by taking images in different wavelength band. Landsat-8 is able to produce image in 11 bands and this performance domain provides scientists better understanding of the progress and loss of every element such as vegetation, water and so on. Here, the city Hamburg, Germany, and its surroundings are analysed so that the features are well distinguished by analysis of greyscale image, histogram, false color image, cluster classification and scatter plot.

Keywords: Landsat-8, OLI, TIRS, Satellite imaging, Supervised classification, Unsupervised classification, K-Means algorithm

INTRODUCTION

The intentions of the Earth observation projects can be explained in different fields of science from the Earth Science to Politics. National space forces take advantage of spy satellites to provide politicians real-time observations of strategic coordinates. Also, scientific community needs to observe the Earth's surface to evaluate any changes in the environment. For instance, Landsat data have been used in a variety of government, public, private, and nationality security applications such as land and water management, global change research, oil and mineral exploration, agricultural yield forecasting, pollution monitoring, land surface change detection, and cartographic mapping (USGS 2019).

LANDSAT SERIES

A continuous series of land remote sensing satellites began in 1972, and the Landsat-8 is the latest in this series. The first satellite had two Earth-viewing imagers on-board: Return Beam Vidicon (RBV) and an 80-meter 4-band Multispectral Scanner (MSS). Although Landsat-2 and Landsat-3 were configured similarly, the fourth satellite carried a new instrument called the Thematic Mapper (TM) as well as MSS. Then, Landsat-5, a duplicate of Landsat-4, returned scientifically viable data for 28 years. But, Landsat-6 equipped with a 15-meter panchromatic (Pan) band, failed to achieve orbit in 1993. In 1999, Landsat-7 was launched and performed nominally until the failure of the Enhanced Thematic Mapper Plus (ETM+) sensor's Scan Line Corrector (SLC) in May 2003 (USGS 2019). Finally, the collaboration of the Department of U.S. Geological Survey (USGS) and NASA developed Landsat-8, and it was successfully

launched in February 11th, 2013 from Vandenburg Air Force Base, California (Roy et al. 2014).

The Landsat Project has been providing user community calibrated high-quality moderate spatial resolution data of the Earth's surface (USGS 2019). The goal of Landsat-8 is to enhance the scientific understanding of the Earth's system, and its response to the phenomena caused by anthropogenic and natural factors in different coordinates of the Earth's surface (Irons, Dwyer, and Barsi 2012).

SUN-SYNCHRONOUS-ORBIT (SS-O)

The sun-synchronous-orbit (SS-O) is one of the most common forms of earth orbit for space science missions. Many historic satellites use SS-O such as NIMBUs[1], TIROS[2], COBE[3], SME[4] and LANDSAT. The desirable orbital characteristics of SS-O make it as one of the most frequently used orbits for earth science missions. Since the orbital inclination is nearly polar (96.5 – 102.5 degrees), SS-O provides global coverage at all latitudes (with the exception of just a few degrees from the poles). The position of the line of the nodes remains roughly fixed with respect to the sun's direction, lighting conditions along the sunlit ground track remain approximately the same throughout the mission. In SS-O, satellites pass over any given point of planet's surface at the same local mean solar time. Another benefit of fixed nodes is constant thermal environment due to sun exposure for the satellite remaining the same over the mission life SS-O altitudes can be selected over a range of 200 to 1680km so that satellites can accommodate a wide range of viewing geometries and conditions (Boain 2004).

Landsat-8 has a near-polar (orbiting the earth closer to the poles), sun-synchronous orbit. It has an altitude of 705 km with an equator crossing time at 10:11 AM (the local time for the descending node). The time taken by Landsat 8 to complete one orbit is 98.9 minutes.

[1] The Nimbus satellites were a series of seven Earth-observation satellites launched over a 14-year time period from 1964 to 1978, one of which did not achieve orbit. In total, the satellites provided Earth observations for 30 years and collectively carried a total of 33 instruments, including ozone mappers, the Coastal Zone Color Scanner instrument and microwave and infrared radiometers.

[2] The TIROS Program (Television Infrared Observation Satellite) was NASA's first experimental step to determine if satellites could be useful in the study of the Earth. It proved extremely successful, providing the first accurate weather forecasts based on data gathered from space. It began continuous coverage of the Earth's weather in 1962 and was used by meteorologists worldwide.

[3] The Cosmic Background Explorer (COBE) mission was launched to take precise measurements of the diffuse radiation between 1 micrometre and 1 cm over the whole celestial sphere. COBE revolutionized the scientists' understanding of the early cosmos.

[4] The Solar Mesosphere Explorer (SME) mission objective was primarily to investigate the processes that create and destroy ozone in the Earth's mesosphere and upper stratosphere.

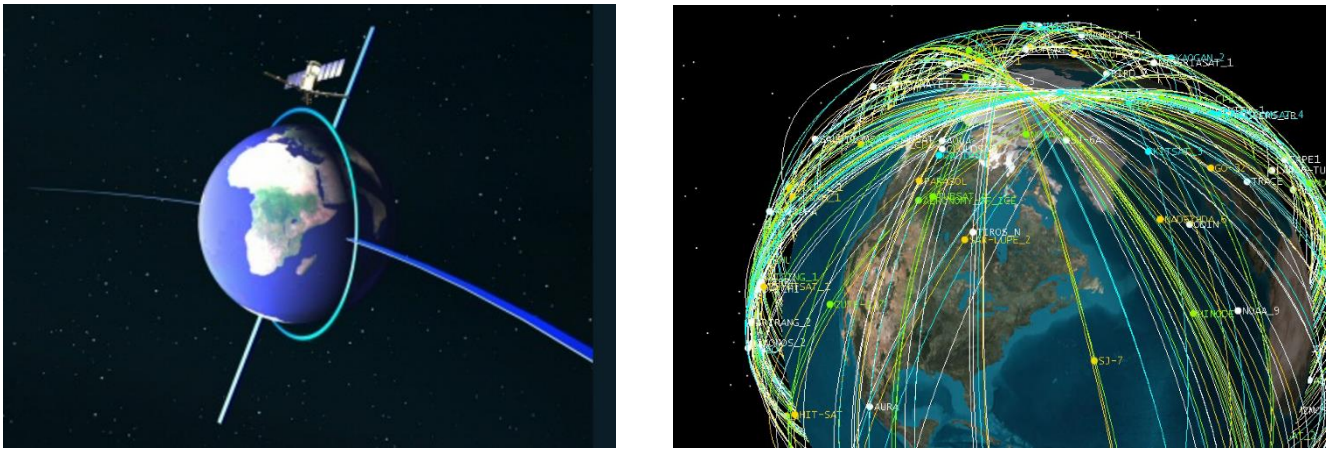

(a) (b)

Figure 1: (a) A satellite orbiting in SS-O (ESA), (b) Sun-Synchronous satellite orbit crossing at the North (Weeden 2008)

OPERATION OF LANDSAT DATA CONTINUITY MISSION (LDCM)

Collecting, archiving, processing and distributing data are the fundamental operations of LDCM. In order to schedule daily data collection, the commands are sent from Mission Operations Element (MOE) to the satellite every 24 hours. The ground system contains the Ground Network Element (GNE) which provides S-band communication between MOE and the satellite. The sensors coincidently collect multispectral digital images of the same Earth's surface areas, and after storing by the spacecraft bus, the data is transmitted to several stations via an X-band data stream from an all-earth omni antenna. A Data Processing and Archive System (DPAS) allows users to search and receive data from the Internet (Irons, Dwyer, and Barsi 2012).

THE ON-BOARD SENSORS OF LANDSAT-8

On-board observatory and the ground system are the two major segments of LDCM. The former consists of the spacecraft bus and the two on-board sensors as its payload: Operational Land Image (OLI) and the Thermal Infrared Sensor (TIRS). Over 500 image scenes per day are ingested using these sensors (Roy et al. 2014). The other sub-systems of Landsat-8 includes data relay systems, attitude-control and orbit-adjustment sub-system, a power supply, and receivers and transmitters as communication sub-system. The sensors are calibrated to better than 5 percent uncertainty in terms of Top of Atmosphere (TOA) reflectance or absolute spectral radiance and have an absolute geodetic accuracy better than 65 meters (m) circular error at 90 percent confidence (CE 90) (USGS 2019).

OPERATIONAL LAND IMAGAER (OLI)

The OLI, built by the Ball Aerospace and Technologies Corporation, takes measurements in the visible, near infrared and short-wave infrared portions of the spectrum. The OLI images have 15 meter (49 feet) panchromatic and 30-meter multi spectral resolution and a 185 km (115 mile) wide swath. Despite covering the areas wide enough, OLI also provides sufficient resolution to distinguish features like urban centres, farms, forests and different vegetation

kinds, rivers and water bodies, other land uses etc. Every 16 days, the entire Earth will fall within the view of OLI due to the near polar orbit of Landsat 8.

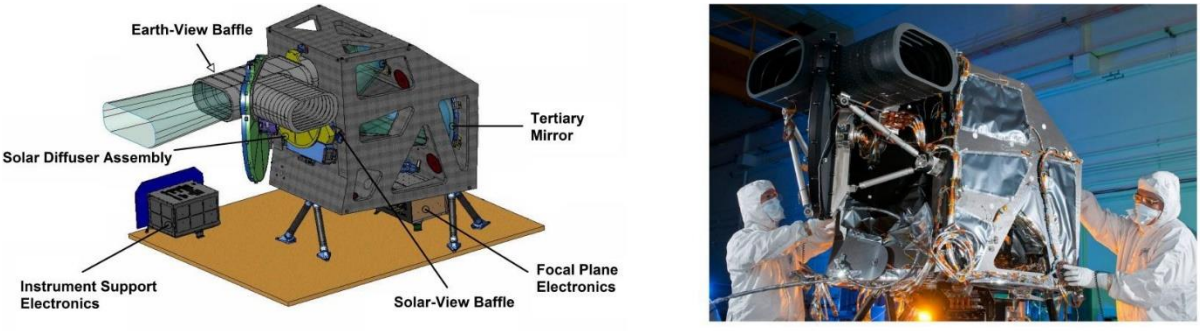

(a) (b)

Figure 2: (a) OLI instrument (USGS 2019), (b) OLI instrument built by the Ball Aerospace & Tecnologies Corporation (NASA 2020)

The OLI sensor collects image data for 9 shortwave spectral bands over a 190km swath with a 30 meter (m) spatial resolution for all bands except the 15m panchromatic band. The widths of several OPI[5] bands are refined to avoid atmospheric absorption features within ETM+ bands. Figure 3 compares the performance of Landsat-7 ETM+ sensor and Landsat-8 OLI sensor according to the atmospheric transmission.

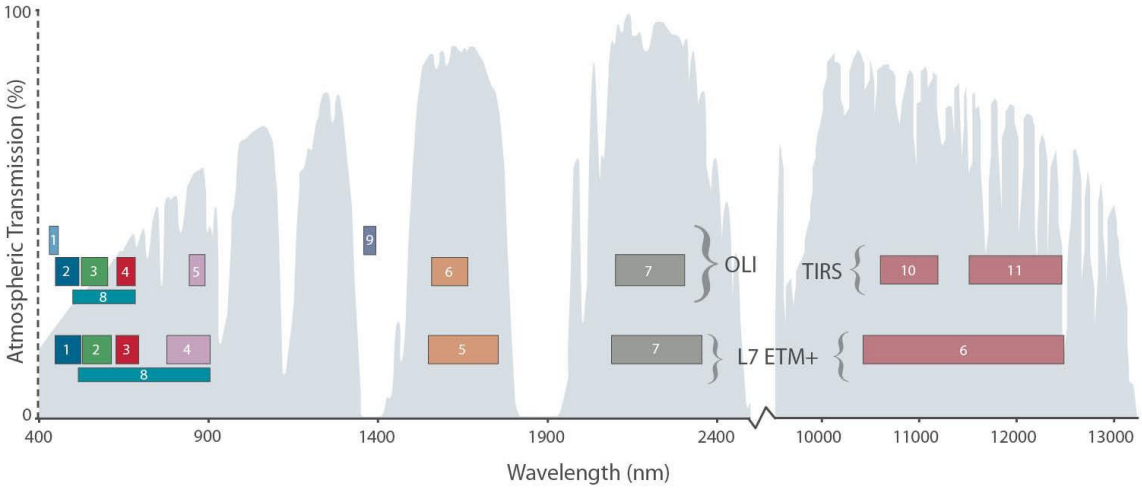

Figure 3: Comparison between ETM+ spectral bands and OLI bands (NASA 2020)

OLI has stringent radiometric performance requirements and is required to produce data calibrated to an uncertainty of less than five percent in terms of absolute, at-aperture spectral radiance and to an uncertainty of less than three percent in terms of TOA spectral reflectance for each of the spectral bands in table 1 (USGS 2019).

[5] Object Pureness Index or OPI is a measure used to assess the integrity of the object in terms of spectral characteristics, and it is based on the standard deviation of multispectral bands, because there is a robust positive correlation between the applied bands (Tavakkoli et al. 2019)

Landsat-7 ETM+ Bands (micrometer)			Landsat-8 OLI and TIRS Bands (micrometer)		
			30m Coastal/Aerosal	0.435 – 0.451	Band 1
Band 1	30m Blue	0.441 – 0.514	30m Blue	0.452 – 0.512	Band 2
Band 2	30m Green	0.519 – 0.601	30m Green	0.533 – 0.590	Band 3
Band 3	30m Red	0.631 – 0.692	30m Red	0.636 – 0.673	Band 4
Band 4	30m NIR	0.772 – 0.898	30m NIR	0.851 – 0.879	Band 5
Band 5	30m SWIR-1	1.547 – 1.749	30m SWIR-1	1.566 – 1.651	Band 6
Band 6	60m TIR	10.31 – 12.36	100m TIR-1	10.50 – 12.51	Band 10
			10m TIR-2	11.50 – 12.51	Band 11
Band 7	30m SWIR-2	2.064 – 2.345	30m SWIR-2	2.107 – 2.294	Band 7
Band 8	15m Pan	0.515 – 0.896	15m Pan	0.503 – 0.676	Band 8
			30m Cirrus	1.363 – 1.384	Band 9

Table 1: Comparison between performance domain of ETM+ and OLI (NASA 2020)

EXPERIMANTAL SETUP

The programming language Python is used to setup the experiment, and a satellite image is displayed with the help of a computer. It does supervised and unsupervised classification in order to analyse different features and different types of vegetation etc. of the land-cover.

The used images are captured by the Landsat-8 satellite, which is a Sun-synchronous near polar orbit satellite which is dedicated in imaging the earth surface. The operational principles of Landsat have been explained above. Therefore, in order to analyse, an image is opened in Python, and then it is displayed for each channel and their histogram. The contrast is enhanced for better visibility and understanding. Further, a false image or an RGB image is created by attaching the colours red, blue and green of the additive colour representation to the three of the channels using the computer program. The chosen channels are NIR, Red and Green. Then, some surface types are clearly identified from the image with the help of an actual map. For instance, a large lake, a forest, urban area or city are found using the program. All pixels of that property are marked in the entire image using the pixel based on supervised classification of the surface types. Even small occurrences of these similar vegetation types can be found anywhere in the image.

PROCEDURE

The following are the procedures involved in the experiment:

- The first process is keeping the system equipped for image processing. Here the software Python programming is used in order to analyse images. Specifically, a web-browser based python frontend called Jupyter notebook is used and the program is made ready which we modify accordingly along the process.

- Next step is selecting and crop a suitable region from the whole area. A region of Hamburg containing different types of vegetation and landscapes is chosen.

- For each channel, the channel image is displayed and analysed afterwards.

The following figures display the histogram of the channel image and rescale the lower and upper limits of the histogram dependent on the intensities and obtain the contrast enhanced images and save it in ‘imgscl’.

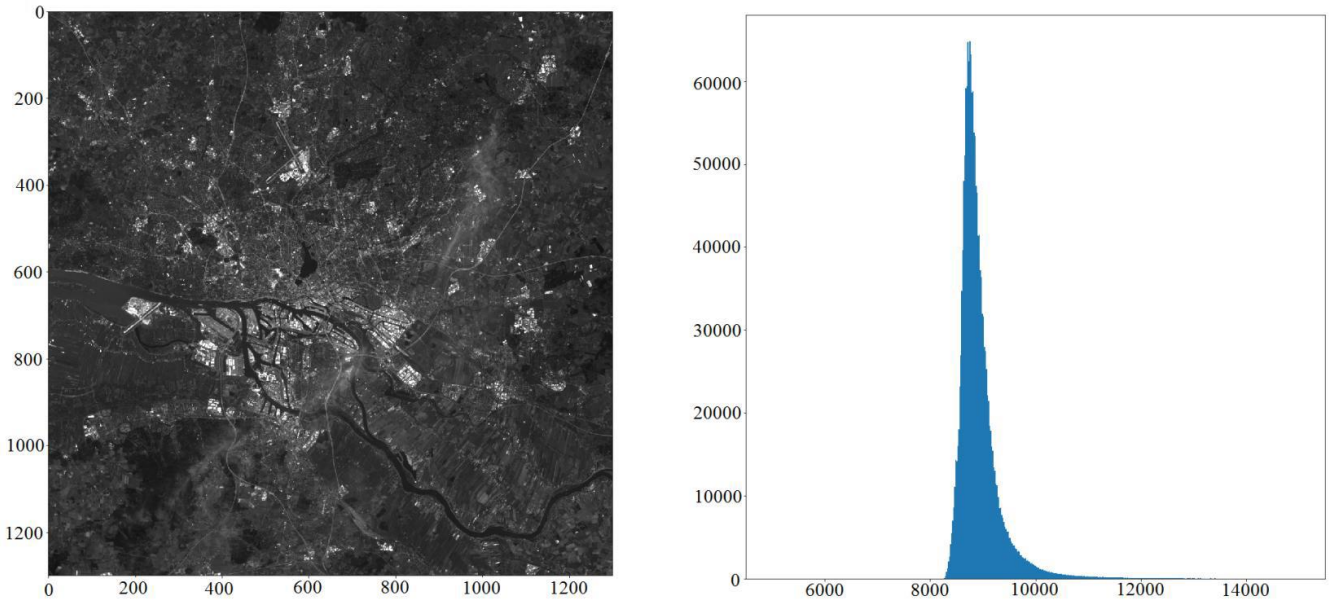

(a) (b)

Figure 4: (a) Greyscale image, channel 0 (ultra-blue), and (b) cropped histogram of the channel 0

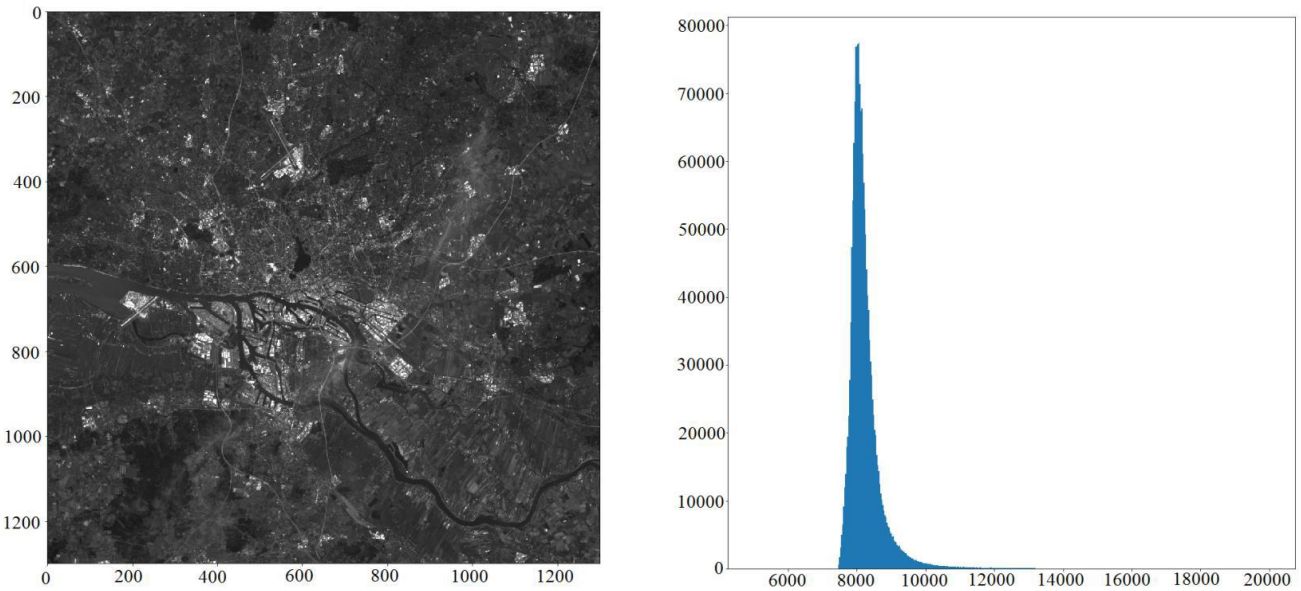

(a) (b)

Figure 5: (a) Greyscale image, channel 1, and (b) cropped histogram of the channel 1

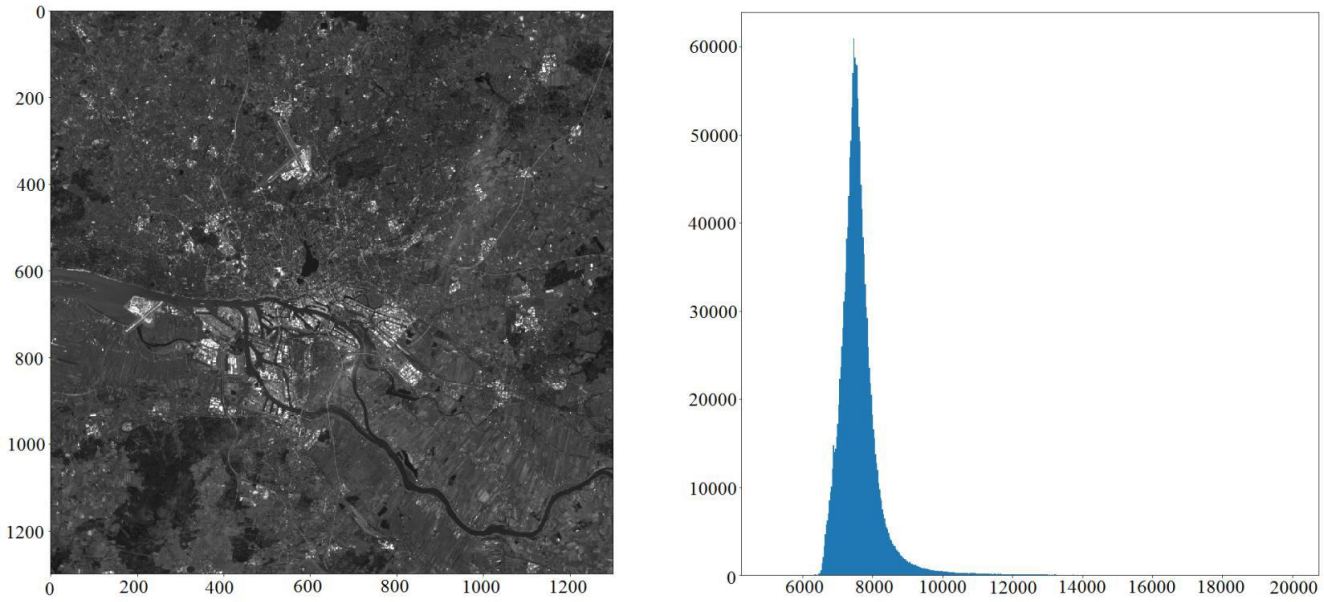

(a) (b)

Figure 6: (a) Greyscale image, channel 2, and (b) cropped histogram of the channel 2

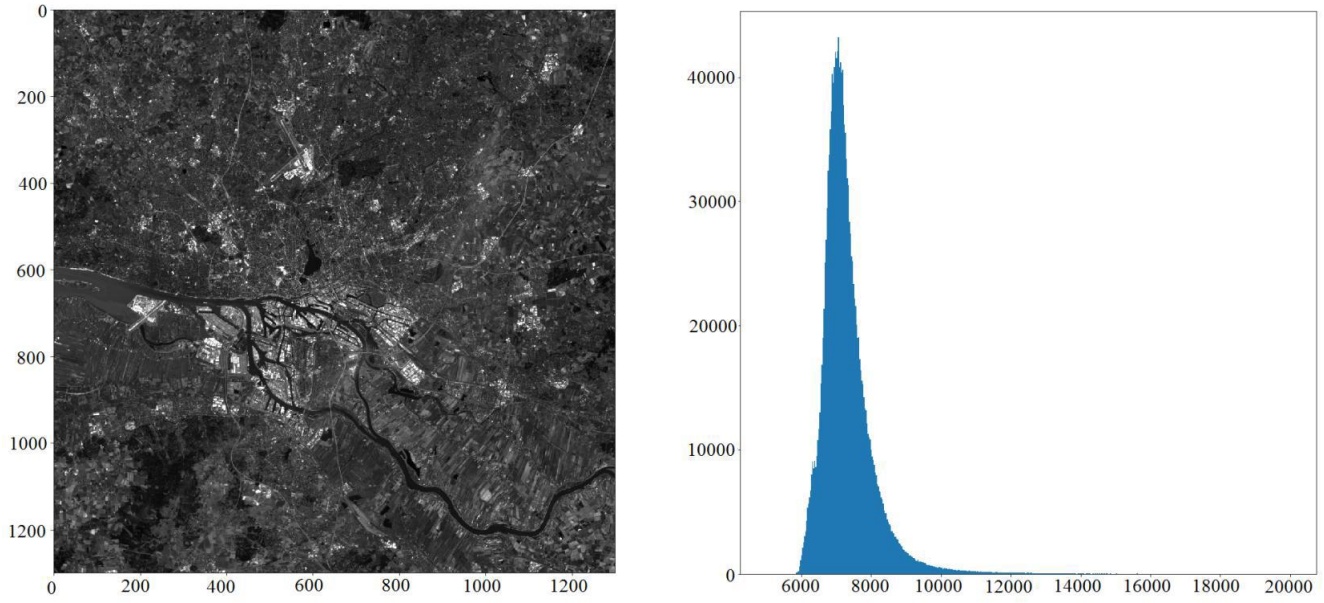

(a) (b)

Figure 7: (a) Greyscale image, channel 3, and (b) cropped histogram of the channel 3

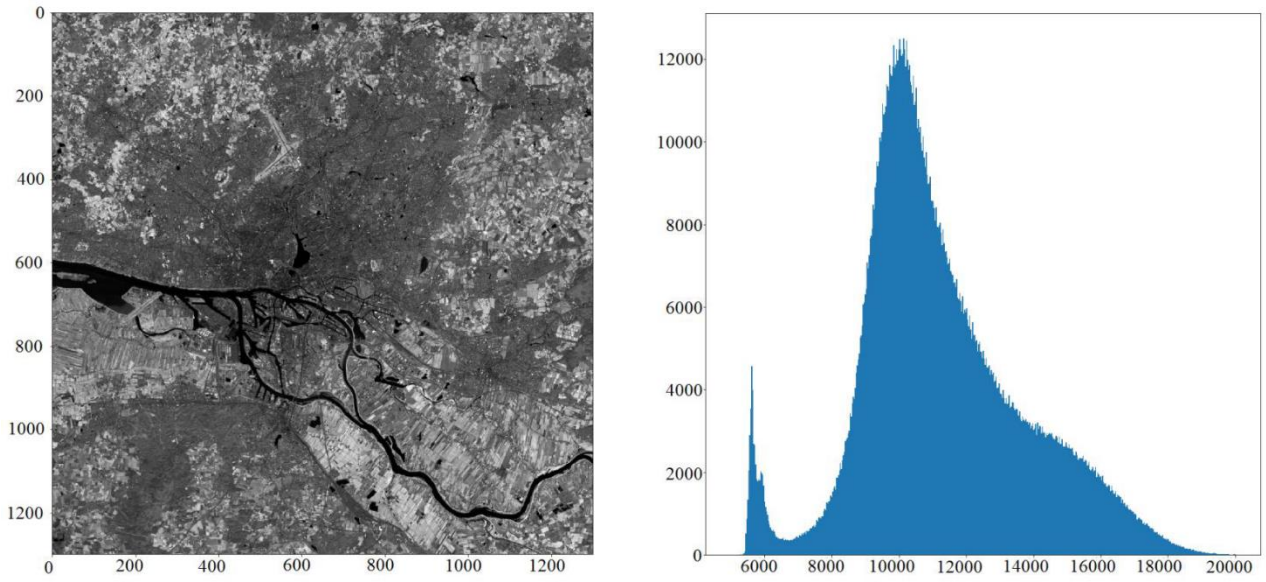

(a) (b)

Figure 8: (a) Greyscale image, channel 4, and (b) cropped histogram of the channel 4

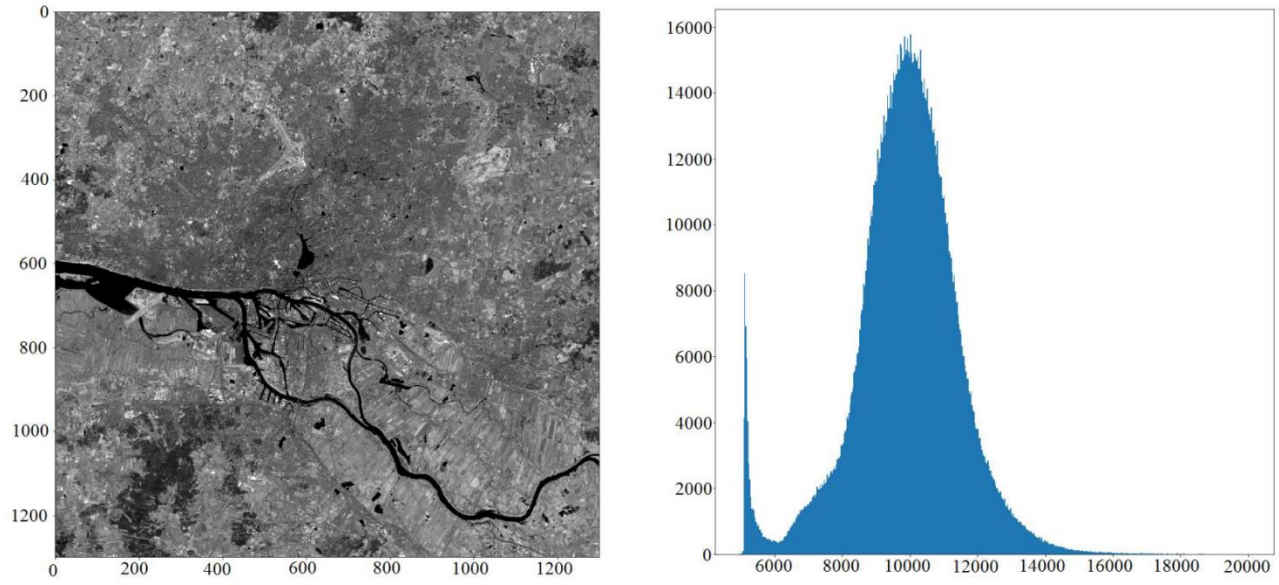

(a) (b)

Figure 9: (a) Greyscale image, channel 5, and (b) cropped histogram of the channel 5

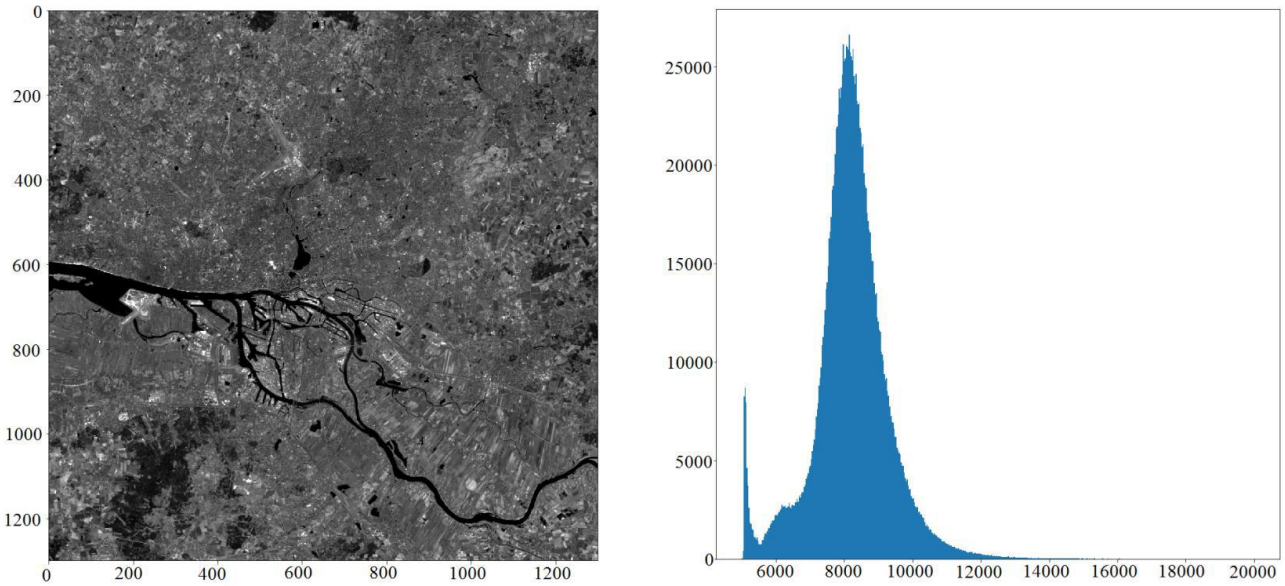

(a) (b)

Figure 10: (a) Greyscale image, channel 6, and (b) cropped histogram of the channel 6

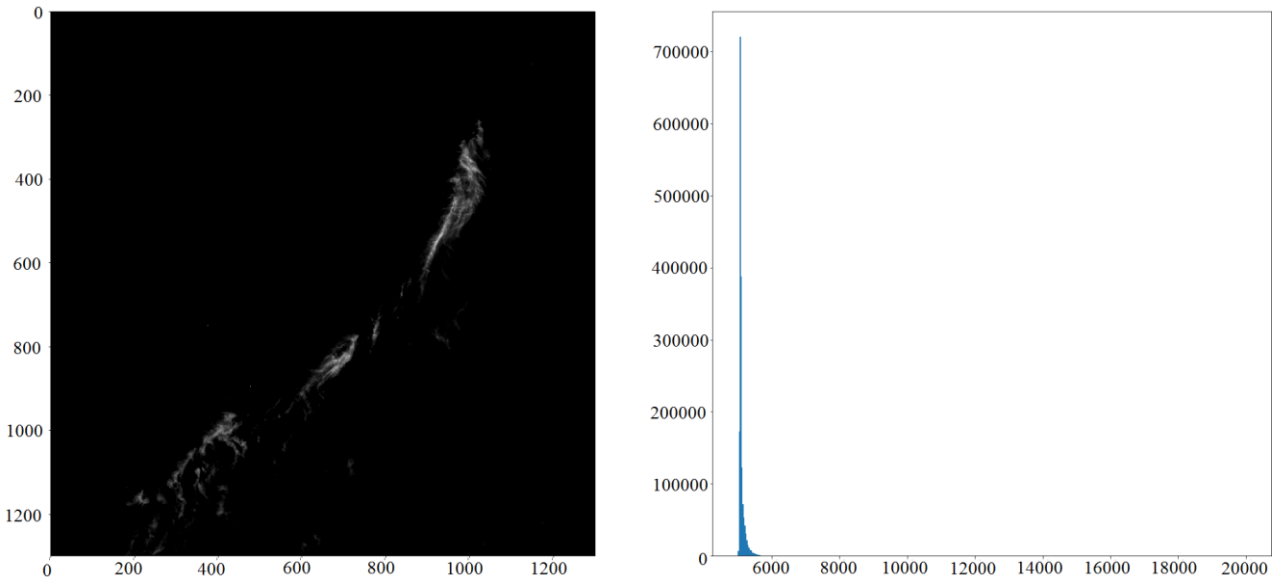

(a) (b)

Figure 11: (a) Greyscale image, channel 7, and (b) cropped histogram of the channel 7

CORRELATION OF CHANNELS

From the images, it is understandable that Blue and Ultra Blue depict approximately the same features. Similarly, Urban and Industrial areas reflect highly in this. Also, water bodies and low vegetation is hard to distinguish in this channel.

Therefore, to extract maximum visible information from the available channels, the linear dependency of the channels or the correlation to one another – the correlation factor is found

out. A correlation coefficient for all the channels is plotted and from this the most and least correlated channels are found.

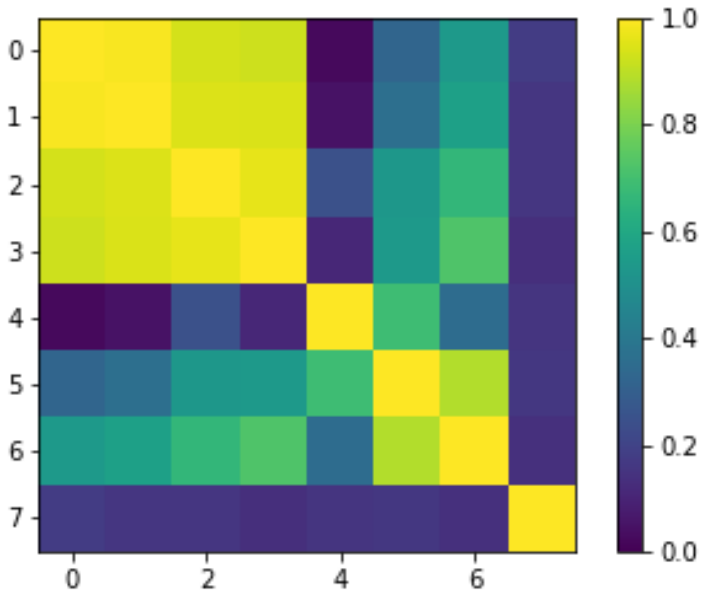

It is evident from the colour bar that channels 0, 1, 2 and 3 are most correlated (Close to 1) and The NIR has the least correlation to other channels. So, to represent with multiple channels, we choose the ones with least correlation within themselves to use for classification. Therefore, we picked the channels 2 (Green), 3 (Red) and 4 (NIR).

A false colour image is generated. It is attached to the colours red, blue and green of the additive colour spectrum normally used in computers to three of the eight channels. The channels are chosen in such a way that the maximum details are visible i.e. the ones with least correlation. Conventionally, the pixels with much vegetation are used to be visible in red. The following combination has been selected.

Channel	**Colour**
4 (NIR)	R
3 (Red)	G
2 (Green)	B

Table 2: The false colour image is generated according to the combination of channels

In the figure 12, most of the vegetation is visible in red. The areas in dark colours resembling black, denotes water bodies and the ones resembling grey denotes the urban areas.

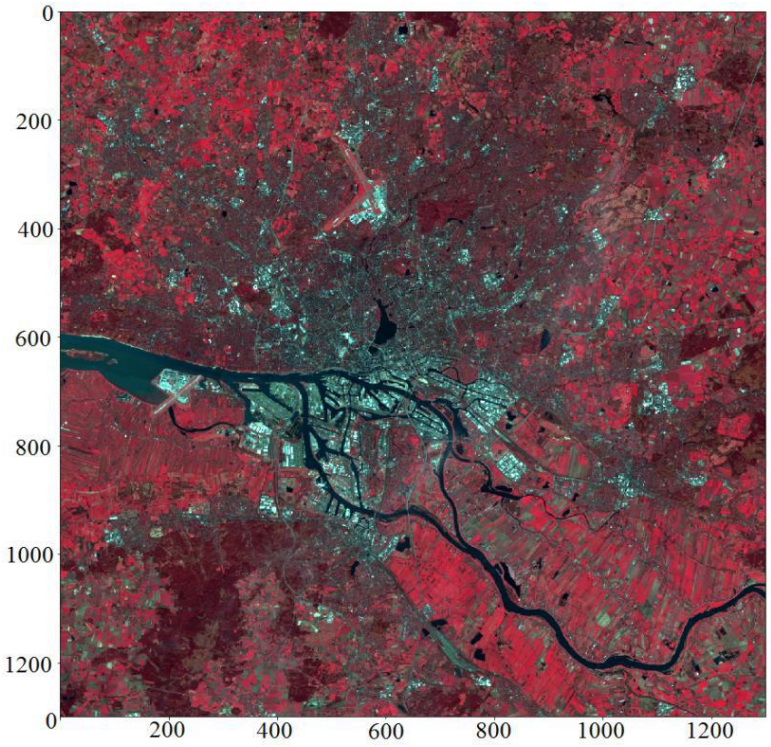

Figure 12: False color image using channels 4(NIR), 3(Red) and 2(Green)

The geographic region of the image is identified on a map by using a suitable maps facility like Google Maps or OpenStreetMap. The displayed regions are marked on the map and the dimensions are stated afterwards. Then, the dimension of one pixel is determined from the map and it is compared with the given data image, and it is analysed.

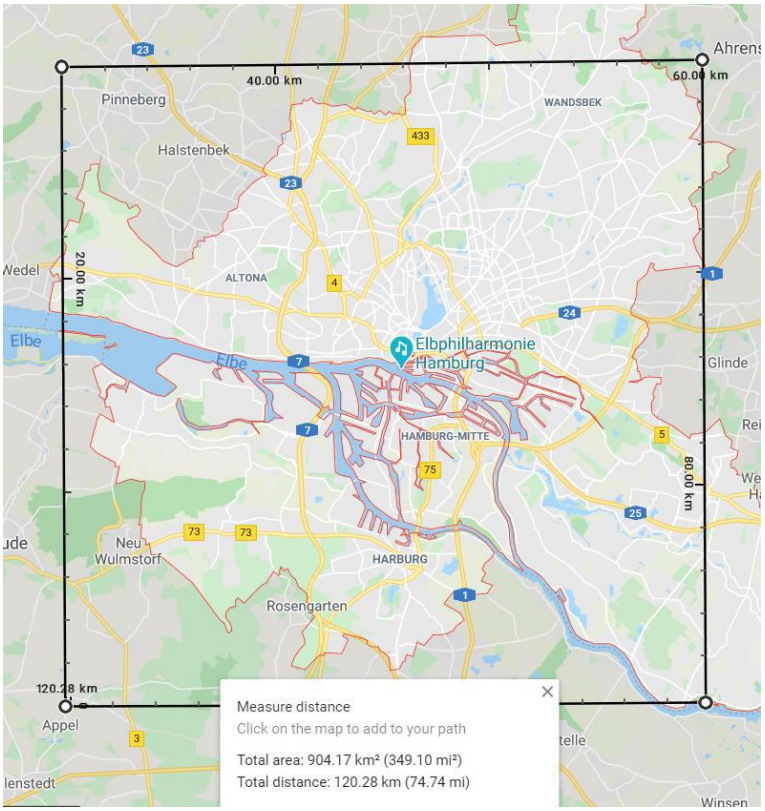

Figure 13: Same area of the image from Google Maps is shown. The area represents the city of Hamburg towards the centre comprising urban areas, with a lake towards the left and the river flowing across. The area covered in the map is approximately 904.17 km² (349.10mi2), and the perimeter is 120.28km (74.74mi).

In the figure 13, the perimeter is found to be 120.28 km, and also the mean is 123.28/4 = 30.07 km. Each 4 sides are added separately, and the perimeter is needed again to be checked for uncertainties. The measurements are as follows for each side: 29.88 km, 30.11 km, 30.05 km and 30.10 km. The new perimeter is 120.14, and the difference or the uncertainty is 0.14 km. Therefore, the mean including uncertainty = 30.07+0.14 = 30.21 km, and the pixel size of Landsat 8 is obtained by the multiplication of 30m and 30m. By adding this, pixel size would be 30021m/1000 for 30.21 m. The spatial resolution is further verified and found to be almost accurate.

The different kinds of surface types are distinguished with details in the false colour image. The yellow circles denote water bodies: here lakes. The arrow denotes the river which flows towards the estuary, which is almost 100 kms in length, and it flows all the way towards the North Sea at Cuxhaven. There is another tiny circle which maps another small lake near the Hamburg city. The areas denoted in green diamonds show the areas of high vegetation. They are areas like forests. Also, the areas in the blue triangles denote the areas of low vegetation like agriculture and cultivational fields. And finally, the areas marked with the white rectangles denote the urban areas where most of the city's industry and construction/infrastructure lies.

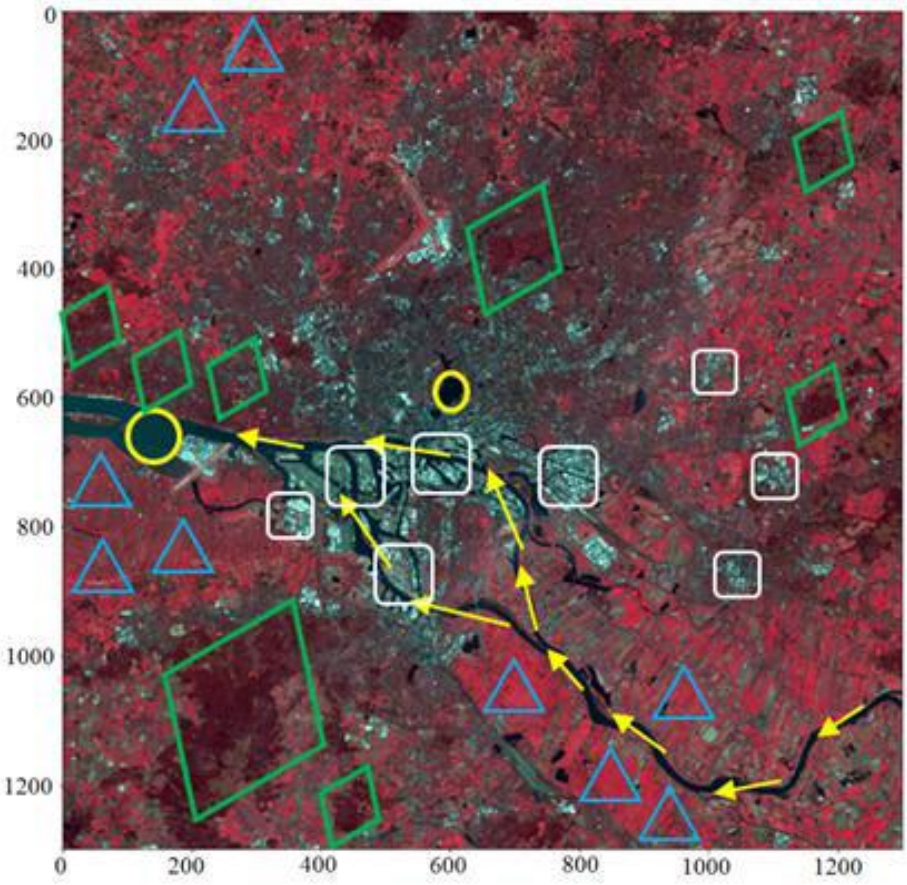

Figure 14: Pixel-based supervised classification of different surface types

Pixel based classification is done using the following steps.

1. Look at the Red / NIR scatter-plot of a uniform area and a known surface type and read the range in the red and NIR that the pixels of this area mainly occupy/ combine ranges from several training areas.
2. Next step is to mark all the pixels in the whole image whose Red and NIR values fall in these ranges. (Here we are colouring them yellow)
3. Do this for each of the other surface types.

From the scatterplot, different surface types are identified. The range of intensities occupied in the Red and NIR channels are identified by using the scatterplot. The lower and upper bound values in the Red and NIR channel are found for each surface type. All the pixels with Red and NIR values within the bounds are displayed within the bounds. The upper and lower bounds for each surface type have been identified from the Red and NIR channels using the scatterplot. For the water areas (Figure15), 3 ranges are taken. Then, classification procedure is applied by using this range, and the following images are obtained. The water areas are marked in arrow in the Figure 14.

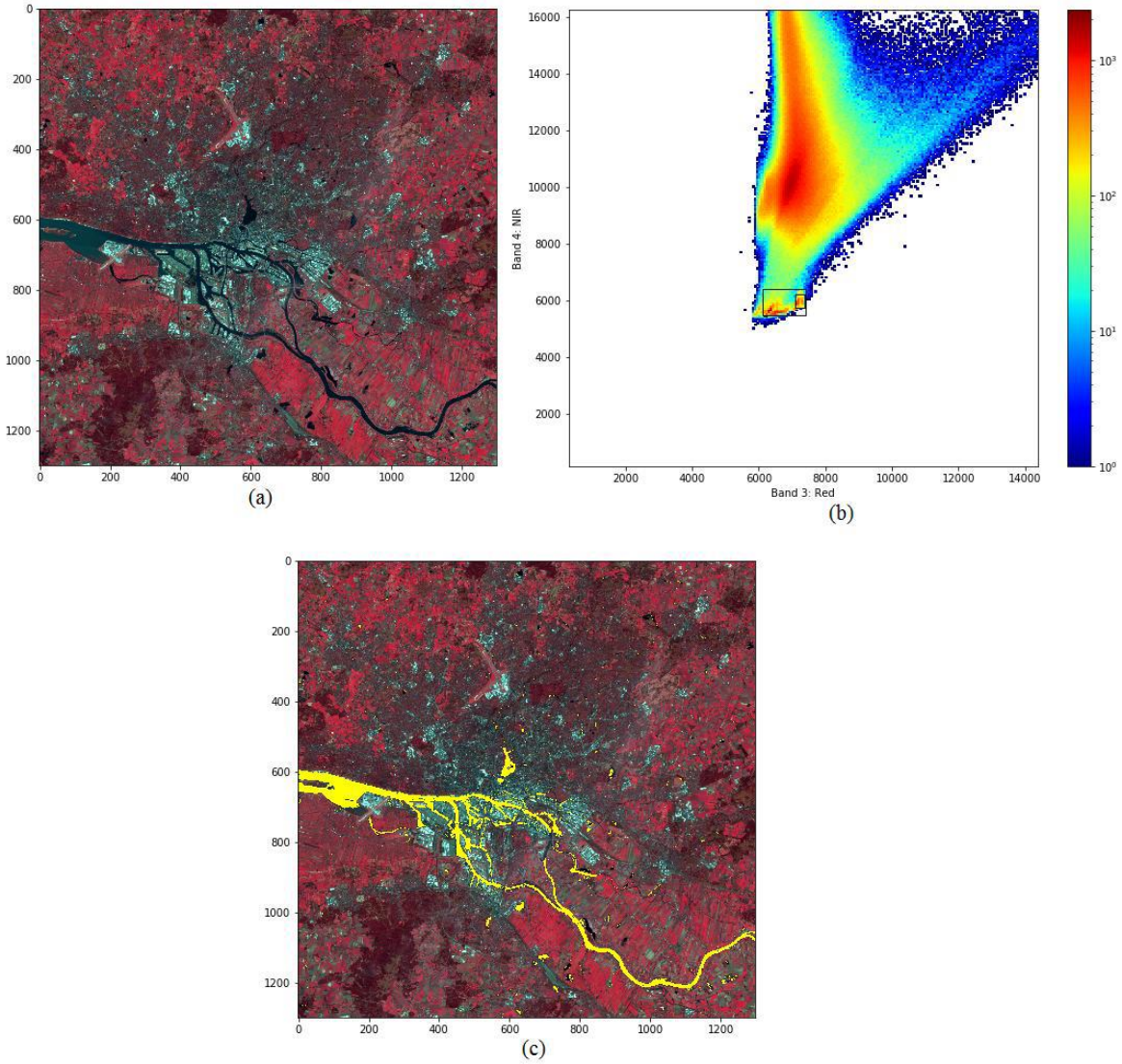

Figure 15: (a) the classification map, (b) the scatter plot, and (c) the range display image of water areas

Similarly, the ranges for each different surface type are found and the classification procedure is applied afterwards. For the urban classification, a range from the central urban area is taken. The following results are obtained after classifying. In the figure 15, urban areas are marked in rectangle.

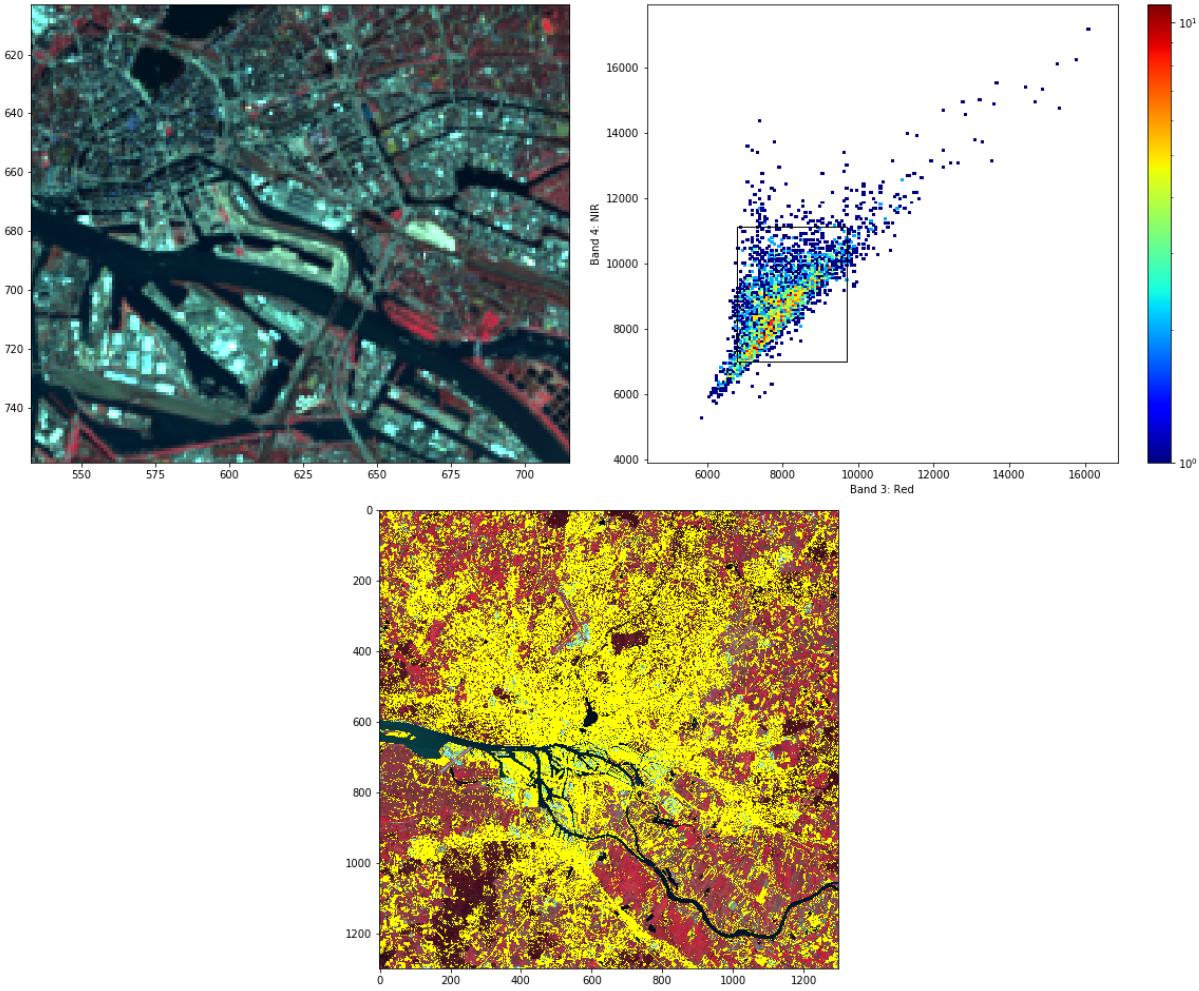

Figure 16: (a) the urban classification, (b) the scatter plot, and (c) the range display image of urban areas.

For the High Vegetation classification, a range from the area is taken that is supposed to have abundant vegetation. Since the data has been obtained in April, the trees are not with much leaves at this time of the season. But, the result seems to be quite accurate to an extent. They are displayed in the Figure 17.

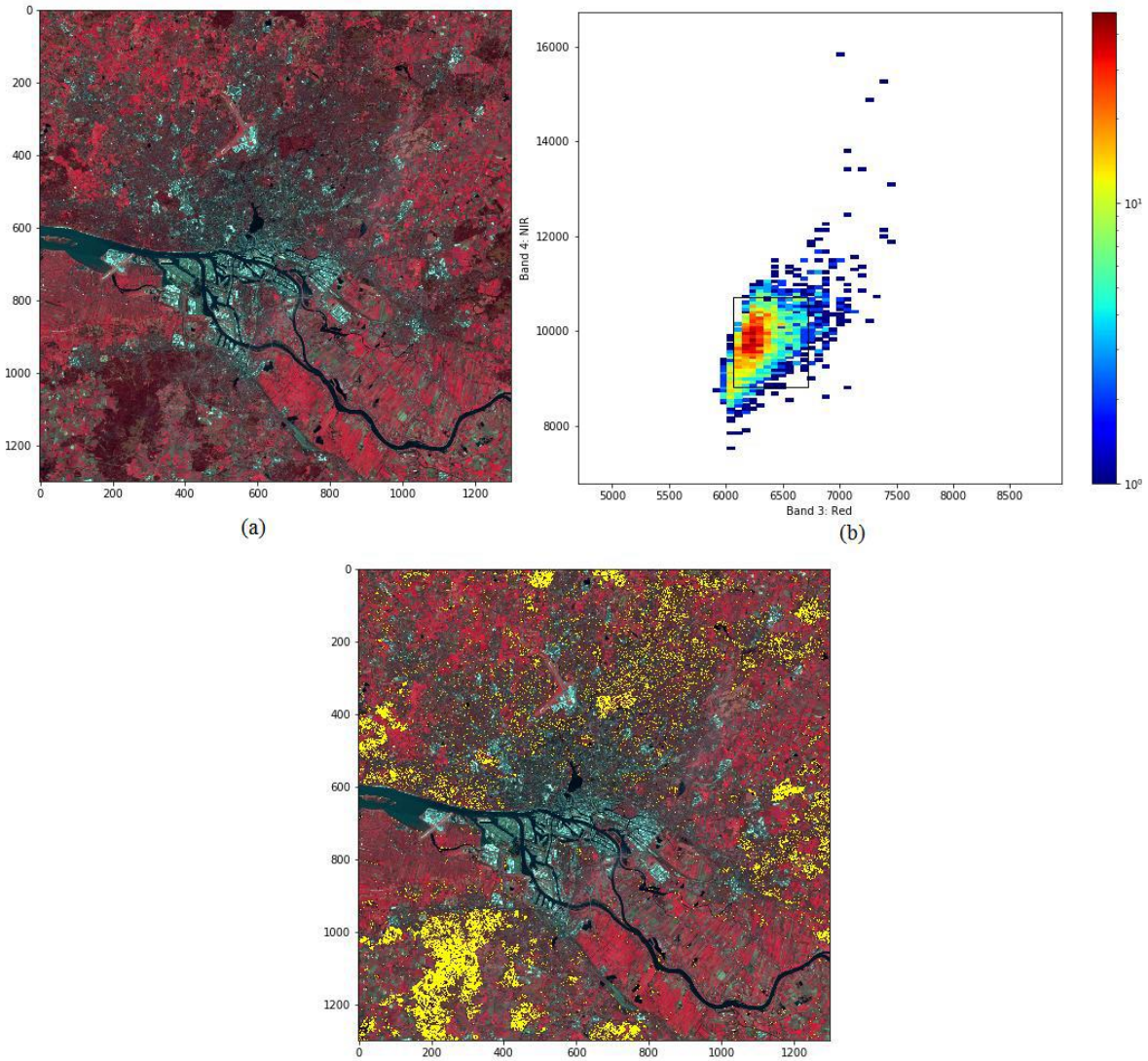

Figure 17: (a) the false colour image, (b) the scatter plot, and (c) the range display image

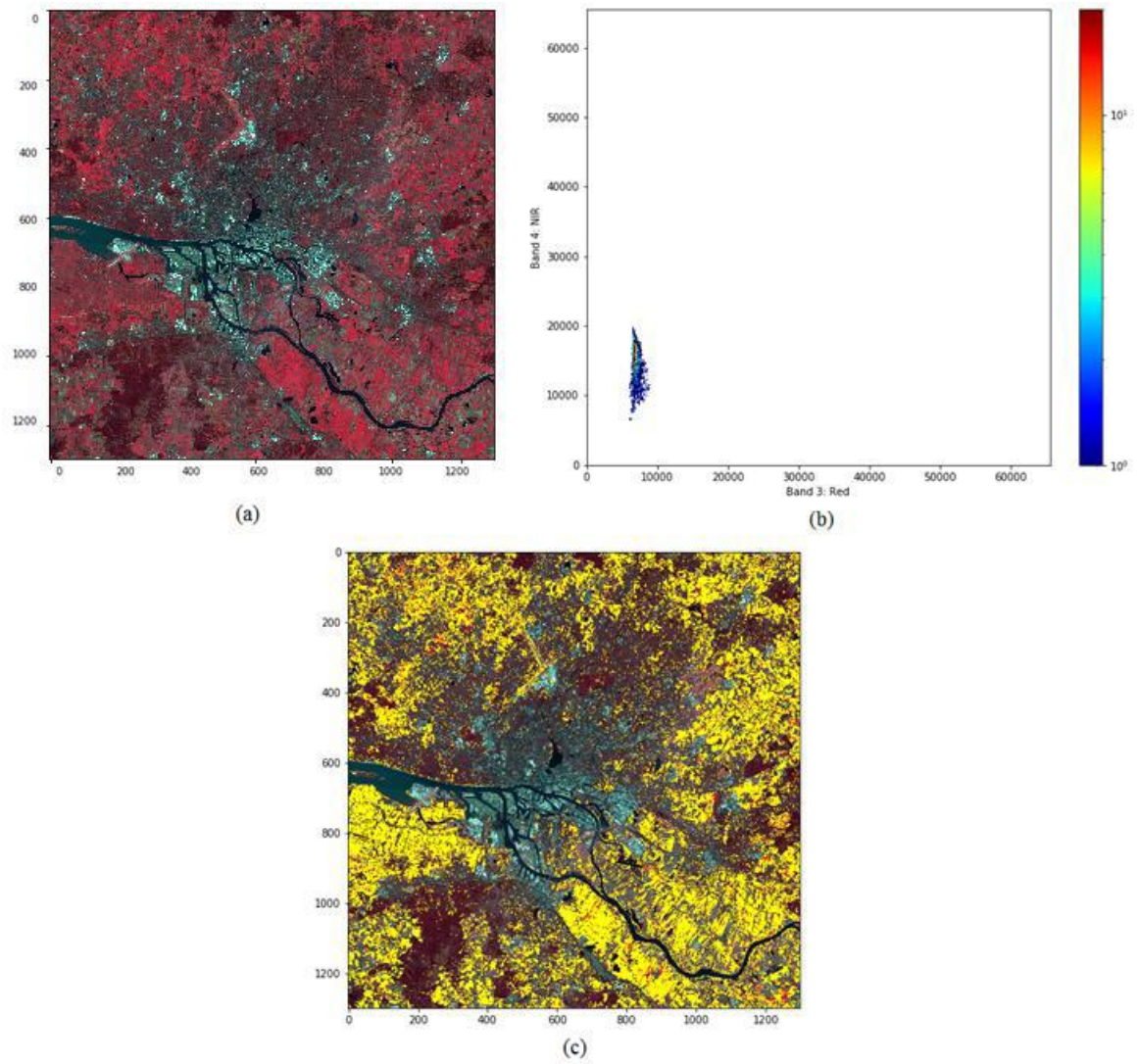

Figure 18: (a) the false colour image, (b) the scatter plot, and (c) the range display image

For the Low Vegetation classification, we similarly chose a range from the area that is supposed to have vegetation that is not so high such as grass and bushes.

From Table 3, it is evident that water appears very darker in both Red and NIR channel. It happens to be on the lower left of the scatter plot, and it can be easily distinguished from other areas. Urban areas are moderately bright in NIR but less bright in Red. It lets to a mistaken with high vegetation which shares similar ranges in the scatter plot. Also, high vegetation seems to be moderately brighter in Red but much brighter in NIR, almost the same as urban areas and this can add some confusion in the areas where they exist. Finally, low vegetation seems to be dark in Red channel but very bright in NIR. It can be distinguished to a greater extent.

	Water		Urban		High Vegetation		Low Vegetation	
	Low	High	Low	High	Low	High	Low	High
Channel 3 Red	6102	7397	6796	9691	6067	6720	6661	7547
Channel 4 NIR	5446	6400	7011	11142	8811	10716	11458	17786

Table 3: The information about the classification of water, urban, high and low vegetation

PIXEL-BASED UNSUPERVISED CLASSIFICATION

In pixel-based unsupervised classification, a cluster algorithm is used to see if the results from supervised (manual) classification match the one from the algorithm. It helps to identify which classification strategy is more effective. Then, the algorithm 'K-Means algorithm' is used. It tries to find the local maxima of densities in the scatterplot of the image and then classifies the whole image accordingly. The cirrus band uses a wavelength where the atmosphere is not transparent because of absorption by water vapor. Therefore, radiation reflected from the surface hardly reaches the instrument.

In the figure 20, a four-cluster classification was carried out, but the results seem to be erratic. It fails to identify the water masses effectively. Similar situation happens with to the urban areas, and also the vegetation is identifiable, even though it contains both high and low vegetation at most parts. The four clusters are obtained by doing K-Means algorithm and the scatter plot of the same is shown is the Figure 20. From the very first look, it is evident that this is not precise. For instance, the water bodies are combined with low vegetation and a bit of urban areas in cluster 4.

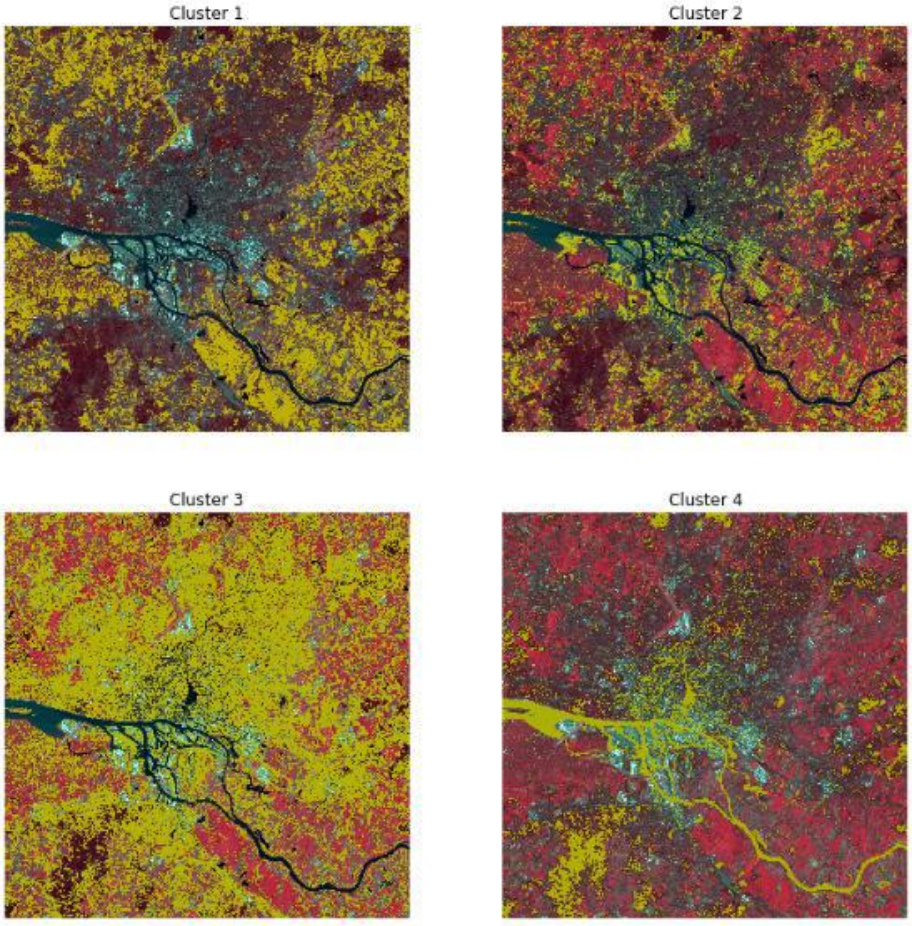

Figure 19: Four cluster classification

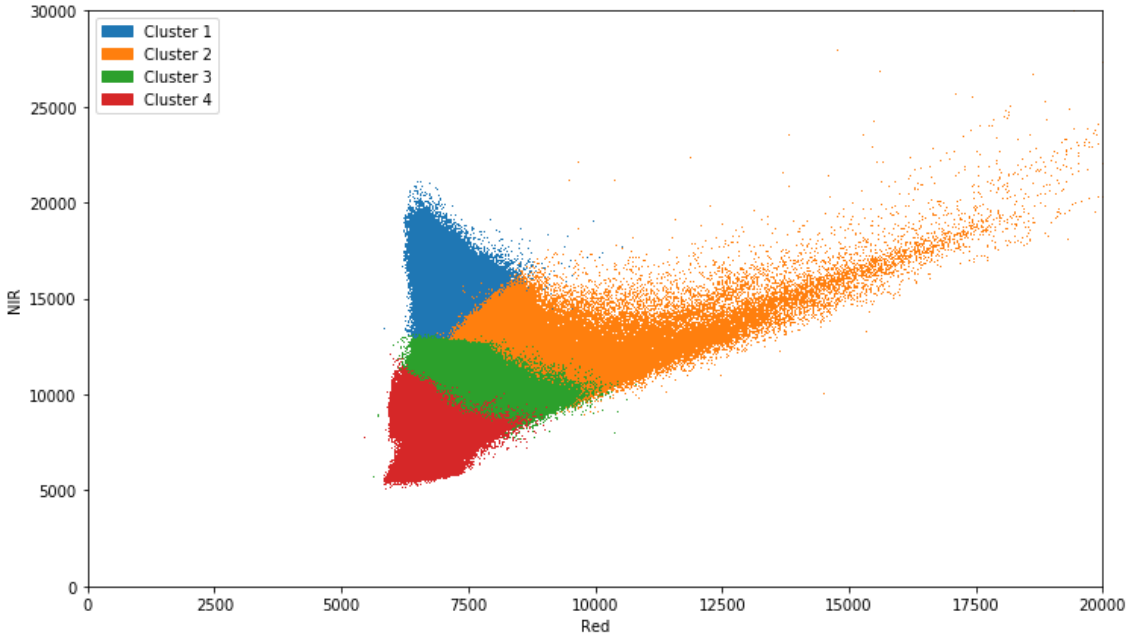

Figure 20: The scatter plot of the four classifications in Figure 19

Since the results are not matched to the supervised classification did manually, this is calculated again with five clusters this time using the K-Means algorithm.

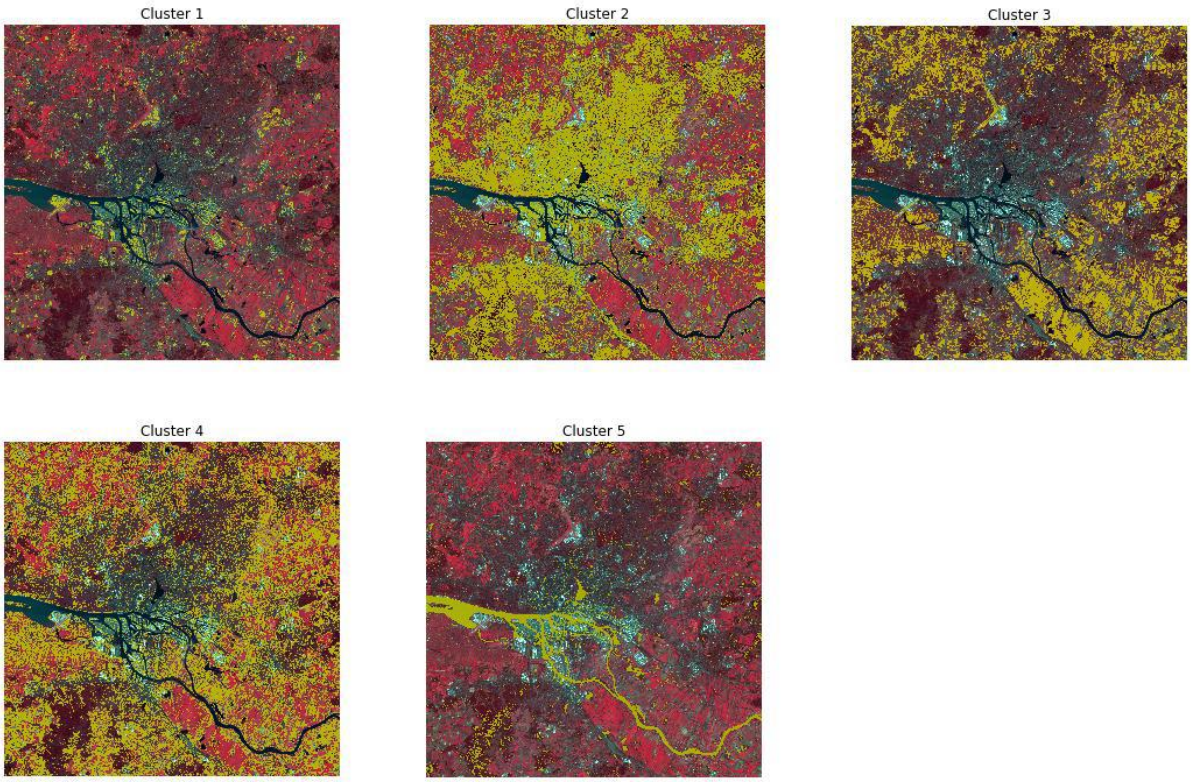

Figure 21: Five cluster classification and scatter plot

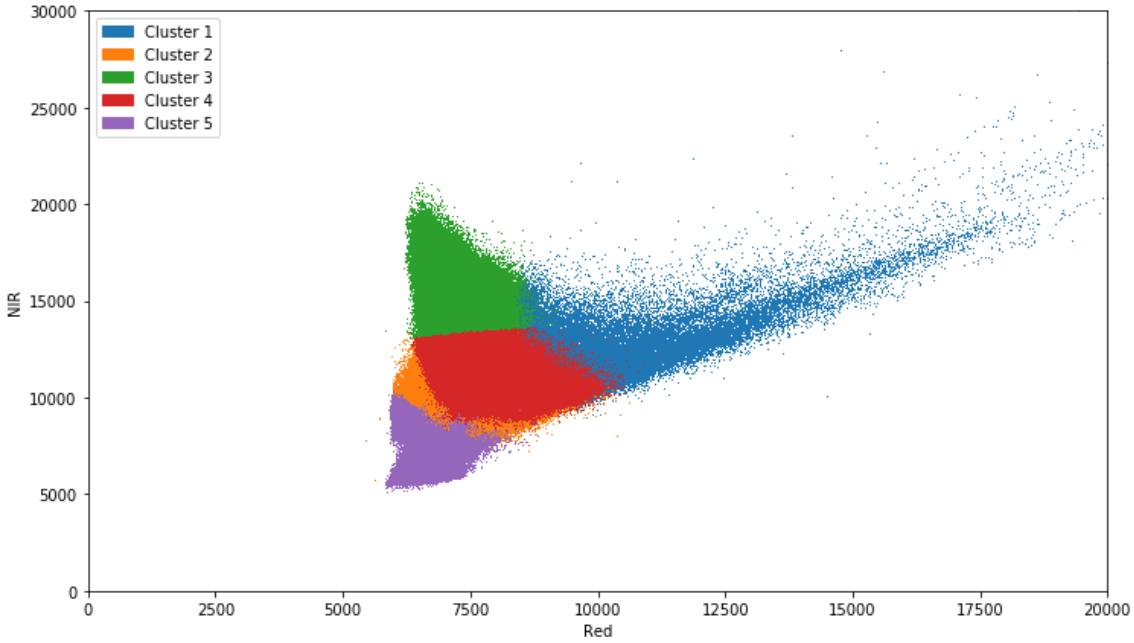

Figure 22: The scatter plot of the five classifications in figure 21

From the scatter plot in the Figure 22, it can be identified that even though the five-cluster classification is better than the 4-cluster one, it tends to reduce or squeeze cluster 5 more, but has done a decent job in identifying water. Clusters 3 and 4 denote vegetation. The former is bright (low veg.) and the latter contains high vegetation. Cluster 2 denotes the urban area here with accuracy almost at par with supervised classification except it doesn't include some high vegetation. Cluster 1 denotes the industrial area which happens to be on the very brighter side of the scatter plot. It denotes areas such as the airport, Airbus company, and such huge industries, but some high vegetation areas are also included.

SUMMARY AND CONCLUSION

The aim of this experiment is analysing the satellite image from a Landsat 8 to analyse the image and do a supervised and unsupervised classification. The chosen region is the city Hamburg in Germany. The reason behind this is that Hamburg is diverse in land-cover. It possesses water bodies, rivers crossing the city, urban areas, huge industrial lands, airport and Airbus company, and both thickly vegetated areas and low vegetation.

The main objective here is to create a false colour image from the given satellite image from Landsat 8. Then, the same area is opened on maps and is displayed the same region. The surface types are analysed visually so that both images are compared.

In the false colour image, the bands 4(Infrared), 3(Red) and 2(Green) are only considered. Therefore, the image we get appears to be a mixture of red, dark red/brown, white/grey, and black. The reason is that unlike a true colour image which only visualizes the picture with respect to the colours or wavelengths in the visible spectrum, a satellite imager has far more advanced sensor systems in the OLI and TIRS sensors. The sensors capture the interactions of even the invisible part of the spectra with the object. These surfaces react differently to each wavelength and the gotten image is a combination of all these.

In the false colour combination used here, vegetation appears as red. This can vary from darker-red for high vegetation to brighter red showing low vegetation. This is because green vegetation readily reflects the infrared light energy. The water bodies appear dark or black in this image due to the almost complete absorption of solar radiation by water in the NIR and SWIR and because of the diffuse scattering and absorption of light by the suspended and dissolved matter in water. Therefore, water appears dark in even red, green and even blue channels. In addition, water surface also reflects a minor percentage of the sunlight away by specular reflection. Also, the urban areas and the industries appear in white and grey. Therefore, by producing the false colour image of the satellite image, the following types of vegetation are distinguished: high vegetation, low vegetation, water bodies, urban areas and industrial areas. Then, a pixel-based classification on Red and NIR and the higher and upper boundaries of intensities are found from the scatter plot.

A problem is the chosen period. A Landsat image taken in the April months is analysed, and during this time, trees carry less leaves, as it is just after winter. Therefore, it cannot be as reflective as high vegetation.

During supervised classification, areas are selected, and in order to classify, the ranges are identified from the scatter plot. This is more of a refined approach if it is applied to a known area. Training data are required otherwise to refine the classification of unknown areas.

The main difficulty with the unsupervised classification is that unlike supervised classification, it tries to take values and then fill in the rest in making scatter plot. The unnecessary areas are sometimes left in scatterplot in supervised classification, helping to get a more precise range. However, unsupervised algorithm fails to do this. The classification seems erratic and land-covers seem to be mistakenly mixed up with each other as explained earlier with the images.

Considering the results of the images, it is much easier to distinguish the terrain in supervised classification. In the K-Means cluster algorithm, the land forms are determined by using the computer alone. It is found to be less precise and effective less clusters are chosen but as we incorporate more clusters, the results, despite improving, can get even more complicated and mixed.

REFERENCE

[1] Boain, Ronald J., (2004): “A-B-Cs of Sun-Synchronous Orbit Mission Design”

[2] European Space Agancy (ESA),: The SMOS satellite in sun-synchronous orbit, website visiting date: 01.07.2020 https://www.esa.int/ESA_Multimedia/Images/2018/07/The_SMOS_satellite_in_sun-synchronous_orbit

[3] Irons, J. R., Dwyer, J. L., & Barsi, J. A. (2012): “The next Landsat satellite: The Landsat Data Continuity Mission, Remote Sensing of Environment”

[4] National Aeronautics and Space Administration (NASA) (The last update 5th of June 2020): “Critical Milestone Reached for 2012 Landsat Mission”, website visiting date: 01.07.2020 https://landsat.gsfc.nasa.gov/critical-milestone-reached-for-2012-landsat-mission/

[5] National Aeronautics and Space Administration (NASA) (The last update 5th of June 2020),: Landsat Science, website visiting date: 01.07.2020 https://landsat.gsfc.nasa.gov/landsat-data-continuity-mission

[6] Roy, D. P., Wulder, M. A., Loveland, T. R., Woodcock, C. E., Allen, R. G., Anderson, M. C., Helder, D., Irons, J. R., (2014): “Landsat-8: Science and product vision from terrestrial global change research”

[7] Tavakkoli Piralilou, S., Shahabi, H., Jarihani, B., Ghorbanzadeh, O., Blaschke, T., Gholamnia, K., Raj Meena, S., Aryal, J., (2019): “Landslide Detection Using Multi-Scale Image Segmentation and Different Machine Learning Models in the Higher Himalayas”

[8] USGS (November 2019): “Landsat-8 (L8) Data Users Handbook”, LSDS-1574 version 5.0

[9] Weeden, B., Shortt, K., (2008): “Development of an Architecture of Sun-Synchronous Orbital Slots to Minimize Conjunctions”